Remote Sensing of Environment 160 (2015) 156–165

Contents lists available at ScienceDirect

Remote Sensing of Environment

journal homepage: www.elsevier.com/locate/rse

Evaluating the potential of MODIS satellite data to track temporal dynamics of autumn phenology in a temperate mixed forest

Lingling Liu [a,b,c], Liang Liang [d,*], Mark D. Schwartz [c], Alison Donnelly [c], Zhuosen Wang [e], Crystal B. Schaaf [e], Liangyun Liu [a]

[a] Institute of Remote Sensing and Digital Earth, Chinese Academy of Sciences, Beijing 100094, China
[b] University of Chinese Academy of Sciences, Beijing 100049, China
[c] Department of Geography, University of Wisconsin-Milwaukee, Milwaukee, WI 53201–0413, USA
[d] Department of Geography, University of Kentucky, Lexington, KY 40506–0027, USA
[e] School for the Environment, University of Massachusetts Boston, Boston, MA, 02125–3393, USA

ARTICLE INFO

Article history:
Received 7 May 2014
Received in revised form 28 November 2014
Accepted 19 January 2015
Available online 3 February 2015

Keywords:
Landscape phenology
Land surface phenology
Fall season
Temperate forest
Northern USA
EOS Land Validation Core Site

ABSTRACT

Autumn phenology plays a critical role in regulating growing season duration and can be estimated from satellite remote sensing. However, to date, little work has been undertaken to evaluate the performance of remotely sensed autumn phenology, mainly due to a lack of spatiotemporally compatible field observations. To address this limitation, we conducted intensive ground observations of leaf coloration and leaf fall from 610 deciduous trees at two 625 × 625 m study areas within a mixed forest in northern Wisconsin, USA during 2010 and 2012. We derived landscape phenology (LP) indices by upscaling these plot-level observations to facilitate spatially compatible comparisons with coarse resolution satellite measures. The satellite-derived land surface phenology (LSP) was based on 250 m Moderate Resolution Imaging Spectroradiometer (MODIS) Normalized Difference Vegetation Index (NDVI) and Enhanced Vegetation Index (EVI) data from both standard 16-day composite (MOD13Q1) and daily Nadir Bidirectional Reflectance Distribution Function (BRDF)-Adjusted Reflectance (NBAR) products. The results revealed that LSP dormancy onset differed from the observed date of full leaf coloration by 5.25 days on average (ranging from 0 to 12 days). Furthermore, progression of the autumn season as determined from LSP and LP showed close agreement as increasing LP leaf coloration corresponded to declining NDVI and EVI values. In addition, the end of the leaf coloring phase was marked by a simultaneous stabilizing of both NDVI and EVI time series whereas the timing of the end of the growing season (leaf fall) closely corresponded to minimum NDVI values. These findings clearly support the use of satellite measurements to effectively monitor temporal dynamics of autumn phenology in a temperate mixed forest.

1. Introduction

Plant phenology, the study of recurring life cycle events such as budburst and leaf senescence, is a sensitive bio-indicator of climate change (Ahl et al., 2006; Hughes, 2000; Liu et al., 2014; Richardson, Bailey, Denny, Martin, & O'Keefe, 2006; Schwartz, 1999). Phenological changes can be monitored using: 1) visual observations, 2) ground-based NDVI measurements (Hmimina et al., 2013; Soudani et al., 2012), 3) bioclimatic models (Kang et al., 2003; Schwartz, 1997; White, Thornton, & Running, 1997), 4) visible light digital camera imaging (Richardson, Friedl, Frolking, Pless, & Collaborators, 2011; Sonnentag et al., 2012), and 5) satellite remote sensing. Each of these techniques has advantages and disadvantages, and the choice of method often depends on the questions being addressed and corresponding scale of study. Among these techniques, satellite remote sensing is most useful for large-scale phenological research (Julien & Sobrino, 2009; Zhang, 2001; Zhang, Friedl, & Schaaf, 2006) because it offers global coverage with consistent temporal repeatability, which is not possible with any other data collection methods (Myneni, Keeling, Tucker, Asrar, & Nemani, 1997).

In acquiring accurate remote sensing phenology, considerable progress has been made to develop methods to reduce noise (e.g., cloud contamination) in satellite time series (Chen et al., 2004; Holben, 1986; Jönsson & Eklundh, 2002; Viovy, Arino, & Belward, 1992; Wolfe, Roy, & Vermote, 1998) and to derive and validate phenological markers (e.g., start of season and end of season; Hmimina et al., 2013; Kaduk & Heimann, 1996; Liang, Schwartz, & Fei, 2011; Schwartz, Reed, & White, 2002; Soudani et al., 2008; White et al., 1997; Zhang & Goldberg, 2011; Zhang et al., 2003). In addition to the quality of satellite data, the relevance of the remotely sensed phenology to ground biophysical processes also varies with vegetation type. For example, although phenology of deciduous forests characterized by pronounced seasonal variations can be readily detected by satellite sensors,

* Corresponding author. Tel.: +1 859 257 7058; fax: +1 859 257 6277.
E-mail address: liang.liang@uky.edu (L. Liang).

http://dx.doi.org/10.1016/j.rse.2015.01.011
0034-4257/

evergreen forests show less seasonal variation in foliage color (Moulin, Kergoat, Viovy, & Dedieu, 1997).

To date, most satellite phenology studies have focused on the spring season, and in particular on deriving and validating the start of the growing season (Hamunyela, Verbesselt, Roerink, & Herold, 2013; Liang et al., 2011; Soudani et al., 2008; White et al., 2009). Although the end of the growing season has been estimated with similar methods used for the start of the growing season, the potential of satellite data for accurately monitoring autumn phenology (e.g., leaf coloration and leaf fall) has not been evaluated (Shuai et al., 2013; Zhang, 2001; Zhang & Goldberg, 2011), likely due to a lack of spatiotemporally compatible field data. Given that autumn phenology is important for determining the growing season length and it is also affected by climate warming (Dragoni & Rahman, 2012; Dragoni et al., 2011; Jeong, Ho, Gim, & Brown, 2011), it is important to assess the ability of satellite data to effectively track temporal dynamics of autumn phenology. Such information would permit a more accurate determination of variability in growing season length, which in turn will facilitate a more reliable measure of carbon dynamics in the modeling of vegetation–climate interactions.

Delayed leaf senescence in autumn (as a result of warmer temperatures) has contributed to extensions of the growing seasons in many regions (Donnelly, Salamin, & Jones, 2006; Dragoni et al., 2011; Jeong et al., 2011; Menzel, 2000). Piao, Friedlingstein, Ciais, Viovy, and Demarty (2007) showed that an increased growing season length in the Northern Hemisphere (1980–2002) was due to a combination of an earlier spring greenup and a later senescence in autumn. Similarly, Peñuelas, Filella, and Comas (2002) reported an extension to growing season length in the Mediterranean region over a fifty-year period (1952–2000), resulting from both an earlier starting and a later ending of the growing season. In addition, a number of studies suggested that delays in autumn phenology might have played a stronger role than spring phenology in extending the growing seasons for temperate vegetation over mid- and high latitudes in North America (1982–2006; Zhu et al., 2012), eastern China (1982–1993; Chen, Hu, & Yu, 2005) and over the entire Northern Hemisphere (1982–2008; Jeong et al., 2011).

Both autumn phenology and spring phenology are important for regulating plant growth and biomass accumulation, although with only limited utility to represent the net ecosystem productivity (NEP; Richardson et al., 2010). In addition to the well-recognized importance of spring phenology, several recent studies have emphasized the role of autumn phenology over spring phenology in determining intra- and inter-annual NEP variations of forests (Wu, Chen, et al., 2013; Wu, Gough, et al., 2013). In addition, Taylor et al. (2008) reported that rising atmospheric CO_2 could lead to delayed autumnal leaf coloration and leaf fall for *Populus* sp., highlighting the need for a better understanding of fall phenology for tracking ecosystem responses to climate change. These studies suggest the need to more accurately monitor fall phenology with remote sensing, for which purpose validation using field data is essential.

The performance of MODIS based land surface phenology (LSP) has been mainly limited by the available spatial (250–500 m) and temporal (reduced from daily due to clouds) resolutions (Liang et al., 2011; Schwartz & Reed, 1999; Zhang et al., 2003). To validate LSP, species-specific ground phenology measurements are ideal given their explicit biophysical meaning (Ganguly, Friedl, Tan, Zhang, & Verma, 2010; Schwartz et al., 2002). However, the scale mismatch between traditional phenological observations and satellite pixels makes the direct comparison suffer from considerable uncertainty. Many recent studies have focused on addressing this limitation. For example, Melaas, Friedl, and Zhu (2013) and White, Pontius, and Schaberg (2014) demonstrated the utility of moderate resolution Landsat data as an intermediary to bridge this gap. Networked digital camera measurements also have contributed to this effort by offering economical, objective, and high temporal frequency records of canopy phenology that can be used for validating LSP (Hufkens et al., 2012; Sonnentag et al., 2012). Our previous work used high density visual observations and a landscape upscaling approach to reconcile the scale mismatch while retaining the biophysical meaning of plant phenology for validating LSP (Liang et al., 2011).

As a follow-up effort, the current study is aimed at evaluating MODIS-based autumn phenology using a similar high density in situ data set supported landscape phenology approach (Liang & Schwartz, 2009; Liang et al., 2011). In addition to evaluating the standard 16-day composite vegetation indices (MOD13Q1), the current work also adopted vegetation indices from the daily Nadir Bidirectional Reflectance Distribution Function (BRDF)-Adjusted Reflectance (NBAR). With the high density field data, we intend to evaluate the potential of MODIS data to monitor both the transitional dates and the overall dynamics of fall season forest phenology.

2. Study area and data

2.1. Study area

Our field observation covered two 625 × 625 m study areas (north and south) located near an AmeriFlux eddy covariance tower (Park Falls/WLEF, 45.946°N, 90.272°W) within the Chequamegon National Forest in northern Wisconsin, USA (Fig. 1). This study site is listed as a National Aeronautics and Space Administration (NASA) Earth Observing System (EOS) Land Validation Core Site (Morisette, Privette, & Justice, 2002). The forest in which the study areas are situated, is composed of approximately 30% evergreen and 70% deciduous species with four dominant vegetation types as follows (Burrows et al., 2002; Ewers et al., 2002): (1) upland conifers dominated by red pine (*Pinus resinosa*) and jack pine (*Pinus banksiana*); (2) northern hardwoods consisting mostly of sugar maple (*Acer saccharum*) and other deciduous species such as red maple (*Acer rubrum*), white ash (*Fraxinus americana*), yellow birch (*Betula alleghaniensis*), and basswood (*Tilia americana*); (3) aspen/fir forest, composed primarily of quaking aspen (*Populus tremuloides*) and balsam fir (*Abies balsamea*), and other tree species such as white birch (*Betula papyrifera*) and bigtooth aspen (*Populus grandidentata*); and (4) forested wetlands with white cedar (*Thuja occidentalis*), balsam fir (*A. balsamea*), and speckled alder (*Alnus incana*) being the dominant species. Our two study areas covered these primary vegetation types and included most of the dominant tree species found in the region. In addition, this mixed forest has undergone a transition from carbon source to carbon sink with changes in species composition and forest age (Davis et al., 2003; Denning et al., 2003; Desai, Bolstad, Cook, Davis, & Carey, 2005), therefore providing potential opportunities to relate phenological measurements to carbon flux studies.

2.2. Phenological observation procedures and protocols

We sampled a total of 888 trees (635 deciduous trees – all broadleaf except for eleven *Larix laricina* [tamarack], a needle-leaf species – and 253 evergreen trees) across the two study areas. To facilitate identifying the presence of spatial autocorrelations, we used a 3/7 cyclic sampling scheme (Burrows et al., 2002; Clayton & Hudelson, 1995) along both the latitudinal and longitudinal directions of the transects within each study area (Fig. 1). This sampling scheme optimizes the field work efficiency by using only 3 out of 7 evenly spaced (25 m sampling interval) potential plots to capture consecutive increments of spacing between plots (i.e., 25 m, 50 m, 100 m…). The three largest trees, with preference for dominant species, were identified and tagged at each plot, yielding a total of 864 trees. An additional group of twenty-four *T. americana* (basswood) trees was included in the north study area for comparison with ongoing observations of this species in a small woodlot on the University of Wisconsin-Milwaukee campus (43.081°N, 87.881°W). 25 deciduous trees died during the time of observation, so we focused on the remaining 610 deciduous trees for this study. The evergreen trees

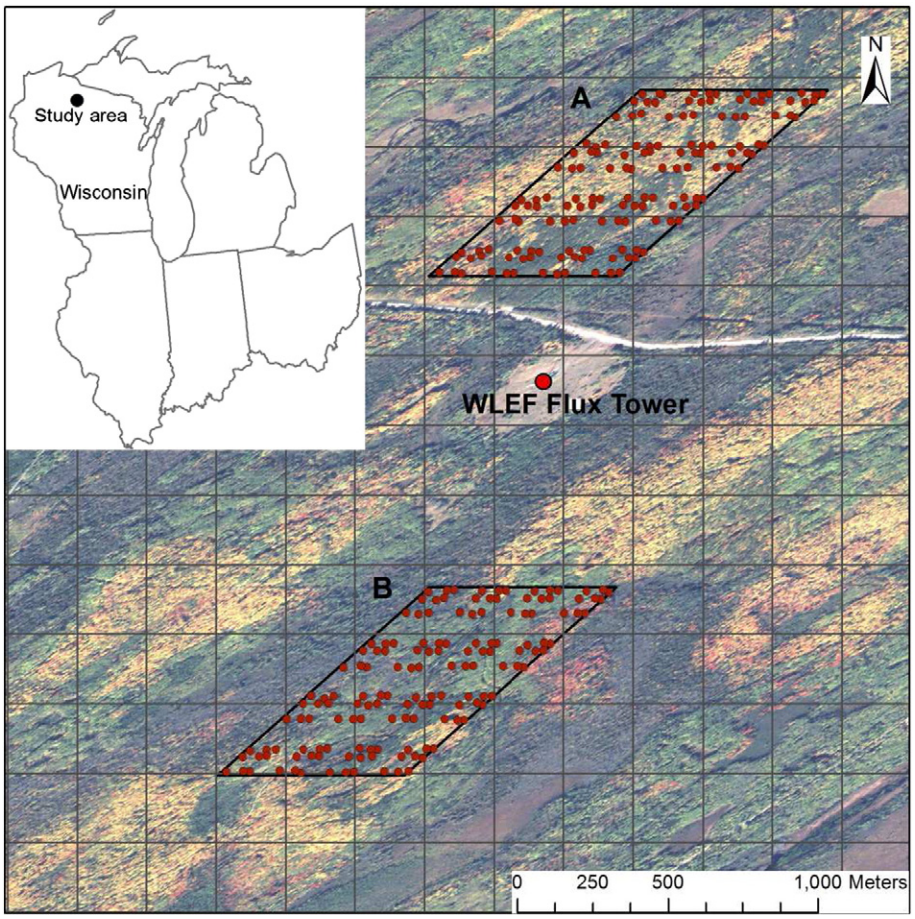

Fig. 1. Study area map (sinusoidal projection) showing: 1) north (A) and south (B) study areas (625 × 625 m) with phenological observation transects/plots; 2) MODIS pixel grids (250 × 250 m); and 3) 2.4 m QuickBird true-color composite (September 27, 2012) underlying the plots and MODIS pixel grids. Inset map shows the location of the study areas within the state of Wisconsin, USA.

were not included in our analysis due to their lack of clearly definable autumn phenophases.

Field observations were conducted over a five-week period from mid-September to late October covering the time of leaf senescence and leaf fall of deciduous trees during 2010 and 2012 (we did not carry out observation in 2011 due to a lack of funding). Phenology of every deciduous tree was recorded every 4 days. The 4-day observation frequency captures rapid phenological change while reducing field work expenses according to our high resolution spring phenology study (Schwartz, Hanes, & Liang, 2013). Due to the limited number of observers, observations were conducted every other day, alternating between the two study areas in order to achieve the 4-day temporal resolution for each study area.

The detailed field protocol used in this study was adapted from those used for weekly phenological observations at the Morgan-Monroe, Indiana AmeriFlux site (J.C. Randolph, personal correspondence), with additions from other protocols and experience gained from the initial (2006) spring field campaign (Burrows et al., 2002, 2003; Meier, 2001; Schwartz et al., 2013). Specifically, a coding system for leaf coloration and leaf fall was designed as follows: 0–10% (800,900), 10–50% (810,910), 50–90% (850,950), and 90–100% (890,990). Whereby '800' represents leaf coloration and the subsequent numbers represent the percentage of leaves that have changed color. Similarly '900' represents leaf fall and the subsequent numbers represent the percentage of leaves that have fallen. For example, a tree canopy with an estimated 50–90% leaf coloration and 50–90% leaf fall is assigned 850 and 950, respectively. Since for most species, leaf coloring and leaf fall occur simultaneously, both the 800 and 900 level codes were recorded to describe the phenological status of a tree for each observation.

2.3. Satellite data

In this study, two typical vegetation indices – NDVI and EVI were used to extract phenological metrics because these two indices are more sensitive to red band increase and greenness decrease (Dragoni & Rahman, 2012; Zhang, Tan, & Yu, 2014) compared to alternatives such as Normalized Difference Water Index (NDWI) which is more sensitive to water content (Delbart, Kergoat, Le Toan, Lhermitte, & Picard, 2005), and Leaf Area Index (LAI) which itself is derived from satellite metrics such as NDVI and therefore possesses additional uncertainties (Kang et al., 2003). Specifically, we used NDVI and EVI data from both the standard 250 m 16-day composite product (MOD13Q1 V005) and the daily 250 m MODIS Nadir Bidirectional Reflectance Distribution Function (BRDF)-Adjusted Reflectance (NBAR) product. The MODIS13Q1 products for 2010 and 2012 were acquired from the Oak Ridge National Laboratory Distributed Active Archive Center (ORNL DAAC: http://www.daac.ornl.gov/MODIS/modis.html). The MOD13Q1 NDVI/EVI values were selected using the Constrained View Angle Maximum Value Composite (CV-AMVC) algorithm over each 16-day compositing period (Huete et al., 2002). The NBAR data retained all available cloud-free data for the study areas as derived off-line with the MODIS daily BRDF/Albedo code run in 250 m mode (Schaaf, Liu, Gao, & Strahler, 2011; Schaaf et al., 2002; Wang et al., 2012, 2014). The daily NDVI and EVI used in this study were extracted from the 250 m MODIS NBAR data.

3. Methodology

3.1. Landscape phenology up-scaling

A nested hierarchical scaling approach was used to integrate spring phenology observations for individual trees and landscape heterogeneity into landscape phenology (LP) indices that are spatially compatible with satellite-based LSP (Liang et al., 2011). In the current study, a similar approach was employed to derive LP indices for autumn phenology by upscaling individual tree phenology to the landscape-level. We focused on the two autumn phenological processes (leaf coloration and leaf fall). Both the time series and phenological markers (full leaf coloration [FLC] and full leaf fall [FLF] dates) at the landscape level were derived through upscaling.

The scaling process/ladder has three critical steps. The first step estimates population phenology by using either spatial interpolation or arithmetic averaging of individual tree phenology. Interpolation was employed when spatial autocorrelation was confirmed to exist for a species on most observation dates. Otherwise, an arithmetic averaging of all individual measurements was used to estimate population phenology on every observation date. The second step involves scaling population phenology to community phenology. Since the presence and abundance of different species within each study area varied significantly, it was necessary to account for variation in community distribution and species composition. The information on community properties were available from our previous study that delineated community boundaries and estimated sub-pixel proportions of deciduous, coniferous, and non-vegetated cover types using high resolution satellite images (i.e. IKONOS and QuickBird; Liang et al., 2011). Community-level phenology was then estimated using a linear transformation of averaged deciduous tree phenology (of dominant species in each community) multiplied by the respective sub-pixel proportions at the pixel level (2.4 m, based on QuickBird). For communities with grass/shrub patches and/or more open canopies, understory phenology was partly accounted for by including speckled alder (a dominant understory shrub in the study areas) as an additional representative species. Finally, landscape phenology was derived by spatially averaging community phenologies for each study area. Given that evergreen trees did not have observable autumn phenology, we only developed the autumn LP indices (leaf coloration and leaf fall) for deciduous trees by weighting the aggregated community phenologies with the total percentage of area occupied by deciduous trees. Therefore the resultant LP indices retained the unit dimension of the phenological protocol used for individual trees.

In addition, we evaluated the sample size effects on LP estimates to provide some logistic guidance to researchers who would like to replicate a high density observation protocol in other vegetated environments, in addition to the suggestions made earlier by Schwartz et al. (2013) for spring phenology. Specifically, we randomly selected a portion of the samples by different percentage levels (from 20% to 90%, with a 10% interval) of the total sample within each study area. For a given sample size, 10 random subset replicates were generated and used to estimate LP for each day. We then calculated the mean absolute error (MAE) from the mean for LP estimates across all observation days and for all replicates at a given sample size. Finally, we produced scatter plots (MAE vs. sample size) for both leaf coloration and leaf fall time series by observation year and study area.

3.2. Deriving land surface phenology

Both the north and south study areas (625 × 625 m) overlapped with twelve 250 m MODIS pixels (Fig. 1). Since neither study area completely covered an entire MODIS pixel, vegetation indices (VI) values of the pixels were first weighted according to their respective percentage of pixel coverage that intersected with the study areas. Then, the area-weighted VI values were spatially averaged to generate a VI value for each study area. For the 16-day composite products, actual image acquisition dates (rather than the beginning dates of composite periods) were used for higher accuracy. Finally, the onset of dormancy in 2010 and 2012 was extracted from both the 16-day composite and daily NBAR NDVI/EVI data using the logistic curve maximum curvature change method (Zhang & Goldberg, 2011; Zhang et al., 2003). The logistic model has been demonstrated to be effective to extract land surface phenology markers from different satellite datasets such as MODIS (Liang et al., 2011; Zhang et al., 2003, 2014), AVHRR (Julien & Sobrino, 2009), and Landsat (Fisher, Mustard, & Vadeboncoeur, 2006; Kovalskyy, Roy, Zhang, & Ju, 2012) and across a variety of ecosystems. This method was also adopted to generate the standard MODIS Global Land Cover Dynamics product (MOD12Q2) (Ganguly et al., 2010). Dormancy onset was defined as the date when photosynthetic activity of vegetation nears zero (Zhang et al., 2003). In addition, the LSP time series used for comparing with the ground observations were derived from daily NBAR NDVI/EVI data corresponding to the time period when ground observations were available.

3.3. Validating land surface phenology

We evaluated LSP using the LP indices for both phenological events and time series of leaf coloration and leaf fall by study area and observation year. To evaluate the accuracy of satellite-derived phenological events, we calculated the absolute error (number of days) between MODIS-based dormancy onset dates and LP-based full leaf coloration and full leaf fall dates. The time series of NDVI/EVI and LP indices (for leaf coloration and leaf fall respectively) were first compared to evaluate the satellite-derived progression of autumn foliage change. Furthermore, we compared normalized daily NBAR VI and LP index values (for leaf coloration only) on all dates with both ground and satellite observations available. VI values were normalized using the formula: (observation − minimum) / (maximum − minimum); LP index values were normalized using a slightly modified formula: (observation − minimum) / (maximum − minimum) × (−1) + 1, given that the autumn phenology protocol values are inversely proportional to canopy greenness. The statistics used for assessing agreement/difference between the two measures included root mean square error (RMSE), coefficient of determination (R^2), and bias. Whereby bias was calculated using the following formula (Soudani et al., 2008):

$$\text{Bias} = \frac{\sum_{i=1}^{N}(\text{LSP}-\text{LP})}{\text{n}}$$

where LSP is a normalized NDVI or EVI value on a certain date for a study area, LP represents a corresponding normalized landscape phenology index value, and n is the number of pairs of LSP and LP measurements for a given year and study area.

4. Results

The departure of MODIS-based dormancy onset dates from the LP-based full leaf coloration (FLC, 890) dates varied from zero to twelve days with a mean absolute error (MAE) of 5.25 days (Table 1). The dormancy onset dates derived from NDVI were mostly earlier than those based on EVI (with one exception in 2012 and the south study area). The NDVI-based estimates were also closer to FLC dates (1–9 days difference and MAE of 3 days), while EVI-based estimates were closer to the full leaf fall (FLF, 990) dates (0–6 days difference and MAE of 3.5 days). There was little difference between NDVI-based dormancy onset and FLC dates whether derived from daily NBAR data or 16-day composite data. However, daily NBAR NDVI-based dormancy onset did show improved accuracy in comparison to the 16-day NDVI based estimates in all cases (MAE: 2.25 days vs. 3.75 days). In addition, estimates of dormancy onset were consistently later than observed FLC dates, except for the north study area in 2012.

Table 1
Dormancy onset dates in day of year (DOY) derived from standard (16-day, MOD13Q1) and daily NBAR NDVI and EVI data, with full leaf coloration (FLC) and full leaf fall (FLF) dates for deciduous landscape phenology (LP) indices in the two study areas for 2010 and 2012.

		Standard 16-day MODIS LSP			Daily NBAR MODIS LSP			Both MODIS products	Ground LP	
		NDVI	EVI	MAE	NDVI	EVI	MAE	MAE	FLC	FLF
2010	North	273	281	5/4	273	283	6/5	5.5/4.5	272	281
	South	276	284	7/4	275	285	7/5	7/4.5	273	279
2012	North	277	279	1/5	278	288	5/5	3/5	279	283
	South	283	275	5/4	279	281	6/1	5.5/2.5	274	280
MAE		3.75/5	5.25/3.5	**4.5/4.25**	2.25/4.5	9.75/3.5	**6/4**	**5.25/4.13**		

Note: 1) The first mean absolute error (MAE) value is between dormancy onset dates and corresponding FLC dates; the second MAE value (in the same field after slash) is between dormancy onset dates and corresponding FLF dates. 2) The bold values are the overall MAE derived from averaging MAE across years, study areas, and VI types. 3) Averaged MAE of LSP derived from the two MODIS products are provided as a general reference of the accuracy of LP.

The LP FLC and FLF dates were several (1–7) days earlier in 2010 than in 2012 for both study areas (Table 1). Compared to the south study area, the north study area had slightly earlier FLC in 2010 and later FLC in 2012 while FLF was later in the north study area in both years. Both daily NBAR and 16-day composite NDVI-based dormancy onset showed earlier dates in 2010 in accordance with the temporal variation in LP, but did not fully agree with LP spatial variation across the two study areas. On the other hand, both daily NBAR and 16-day composite EVI-based dormancy onset estimates agreed with the spatial variation in LP FLC dates across the two study areas each year yet did not show temporal variations that are consistent with LP FLC dates. Furthermore, according to the population level phenology (Table 2), the majority of tree populations showed earlier FLC and FLF in 2010 than in 2012 (except for speckled alder), which was consistent with the interannual variations in LP and NDVI-based dormancy onset estimates.

Comparisons of the LP-based leaf coloration and leaf fall time series vs. daily NBAR VI data are presented in Fig. 2 and 3. During each autumn season, NDVI and EVI values rapidly decreased then stabilized with little change while LP index values first significantly increased (shown as decline to match the change in VI) and gradually leveled off afterwards. The vertical line in each graph provides a visual aid to divide LP time series into a rapid developmental stage and a phase with minimal changes. The increase (shown as decline) in LP leaf coloration and leaf fall values generally corresponded with the decrease in NDVI or EVI values. LP leaf coloration in 2010 showed almost identical timing with the VI time series stabilization (Fig. 2a & b). The time when LP leaf fall time series began to level off lagged behind the VI time series stabilization and corresponded with the minimum NDVI values followed by a slight increase in NDVI in three of the four cases (Fig. 3a, c & d). Furthermore, the normalized LP index values for leaf coloration was significantly ($R^2 > 0.7$, $P < 0.01$) correlated with daily NBAR NDVI and EVI, with relatively small RMSE and bias values (Fig. 4). However, no systematic differences between LSP and LP were identified from the cross-comparison.

In addition, we found that the mean absolute error of LP LF and LC estimates increased rapidly with reduced sample size in the north and south study areas during both 2010 and 2012. The mean absolute errors became relatively small and stable when over 50–60% of the samples were used to estimate LP (Fig. 5). Half (50%) of the current sample size included 137 (south study area) and 168 (north study area) samples from various species. When the percentage was below 10%, certain species were omitted and the mean absolute errors were very large.

5. Discussion

Our study shows that MODIS derived dormancy onset corresponds well with the time of full leaf coloration (FLC) and full leaf fall (FLF) at the landscape level in a mixed forest, demonstrating an explicit link between the satellite derived fall phenological marker and the ground observed fall phenological events. The two simultaneously occurring phenophases (leaf coloration and leaf fall) reached completion consecutively a few days apart (the former being always earlier). NDVI and EVI based dormancy onset estimates matched more closely with FLF (mean absolute errors of 4.13 days) than with FLC (mean absolute errors of 5.25 days). However, given that MODIS VI primarily tracks the leaf chlorophyll content and structure (Wu, Niu, & Gao, 2010), dormancy onset may be more physiologically related to leaf coloration than to leaf fall. Therefore the slightly closer correspondence we found between dormancy onset estimates and FLF dates does not necessarily bear a particular biophysical meaning, yet certainly warrants further investigation. In addition, NDVI-based dormancy onset proved more accurate in predicting interannual variations in FLC than EVI-based dormancy onset which appeared to be able to better capture regional differences in FLC. Although satellite-derived end of the growing season (dormancy onset) showed differences with FLC (0–12 days, MAE 5.25 days) that are comparable to start of season estimates (Hmimina et al., 2013; Liang et al., 2011; Soudani et al., 2008), there seemed to be more inconsistencies with the performance of the two vegetation indices in the fall season. Furthermore, uncertainties with LSP in detecting small spatial and temporal variations in autumn landscape phenology may be caused by more complex surface reflectance variability and greater landscape heterogeneity as influenced by diverse coloration processes of different tree species and a combination of environmental drivers such as temperature, soil moisture, shortening day length, winds, and even spring phenology (Cleland, Chuine, Menzel, Mooney, & Schwartz, 2007). Nonetheless, this and our earlier study focusing on spring phenology (Liang et al., 2011) support the general accuracy of MODIS LSP in detecting both the beginning and ending of the growing season in a mixed forest environment.

Table 2
Ground-based full leaf coloration (FLC) and full leaf fall (FLF) in day of year (DOY) of dominant plant populations (sample size >20, provided in brackets after species name, and standard deviation for each species provided in brackets after FLC or FLF dates) in the two study areas for 2010 and 2012.

Dominant population full leaf coloration (FLC) and full leaf fall (FLF) dates					
North	Year	Basswood (24)	Red maple (83)	Sugar maple (173)	
Study	2010	271 (3.6),274 (5.8)	272 (4.0),280 (5.3)	271 (4.0),281 (4.8)	
Area	2012	274 (2.0),277 (1.4)	274 (3.1),281 (2.8)	274 (2.7),281 (2.1)	
South	Year	Quaking aspen (119)	Red maple (82)	Speckled alder (34)	White birch (23)
Study	2010	273 (3.9),280 (5.6)	271 (3.6),277 (5.1)	278 (9.0),281 (7.7)	271 (3.3),279 (5.5)
Area	2012	275 (4.0),282 (4.0)	274 (3.2),280 (3.1)	276 (6.4),277 (6.2)	273 (3.7),280 (5.9)

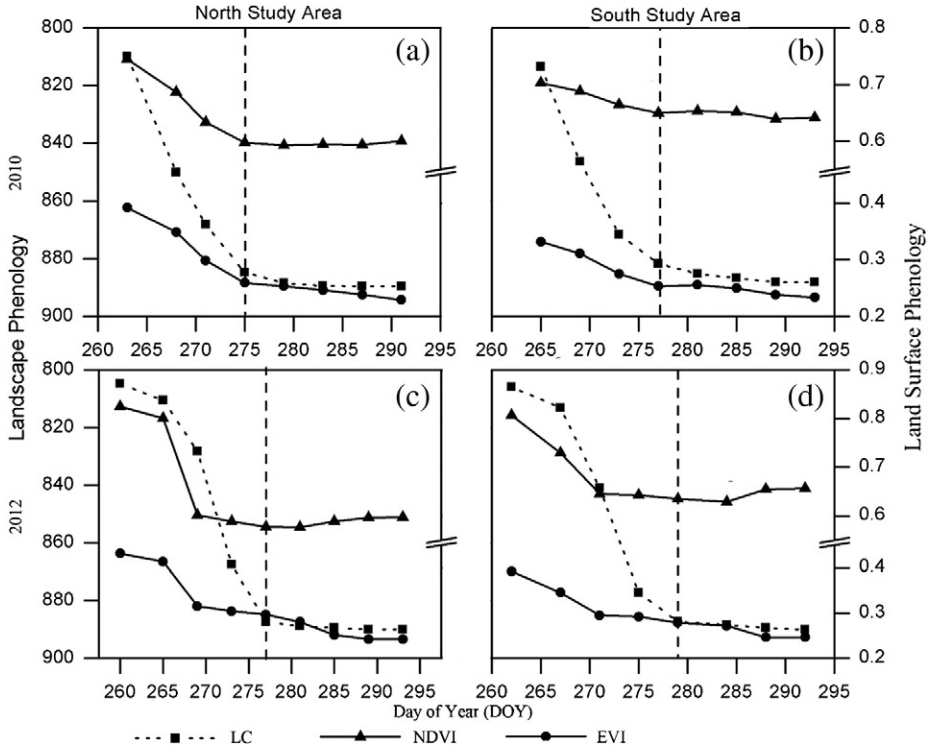

Fig. 2. Land surface phenology/daily VI and landscape phenology index for deciduous leaf coloration (LC) in north and south study areas over the 2010 and 2012 autumn seasons. The LC values are plotted with a reversed direction to match the declining pattern of VI values. A vertical line in each graph provides a visual aid to divide the LP time series into rapid developmental stage and a phase with minimal changes. The break on the right y-axis is due to the value gap between NDVI and EVI for more compact presentation of the curves.

The comparison of daily MODIS NBAR VI data and corresponding high frequency landscape phenology time series helped reveal more detail in the linkages between satellite and ground fall phenology observations. Specifically, the period of rapidly declining NDVI and EVI coincided with an increasing trend in LP index. The dates at which LP leaf coloration increase began to level off more closely matched the time when VI decrease began to significantly slow down, while LP leaf fall increase consistently lagged behind. This strongly suggests that VI

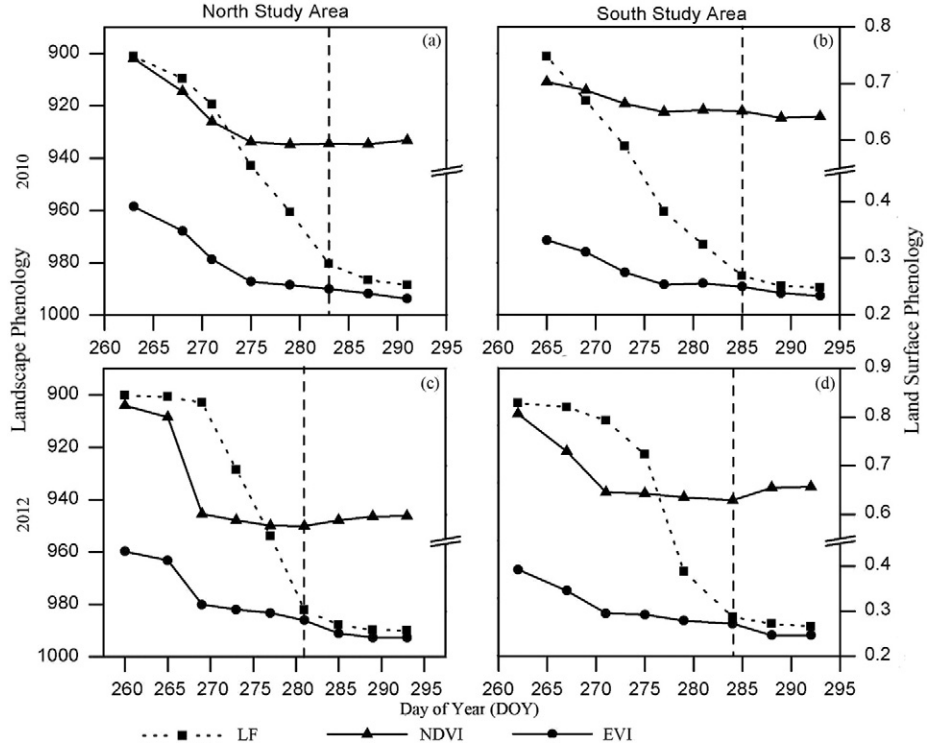

Fig. 3. Land surface phenology/daily VI and landscape phenology index for deciduous leaf fall (LF) in north and south study areas over the 2010 and 2012 autumn seasons. The LF values are plotted with a reversed direction to match the declining pattern of VI values. A vertical line in each graph provides a visual aid to divide the LP time series into rapid developmental stage and a phase with minimal changes. The break on the right y-axis is due to the value gap between NDVI and EVI for more compact presentation of the curves.

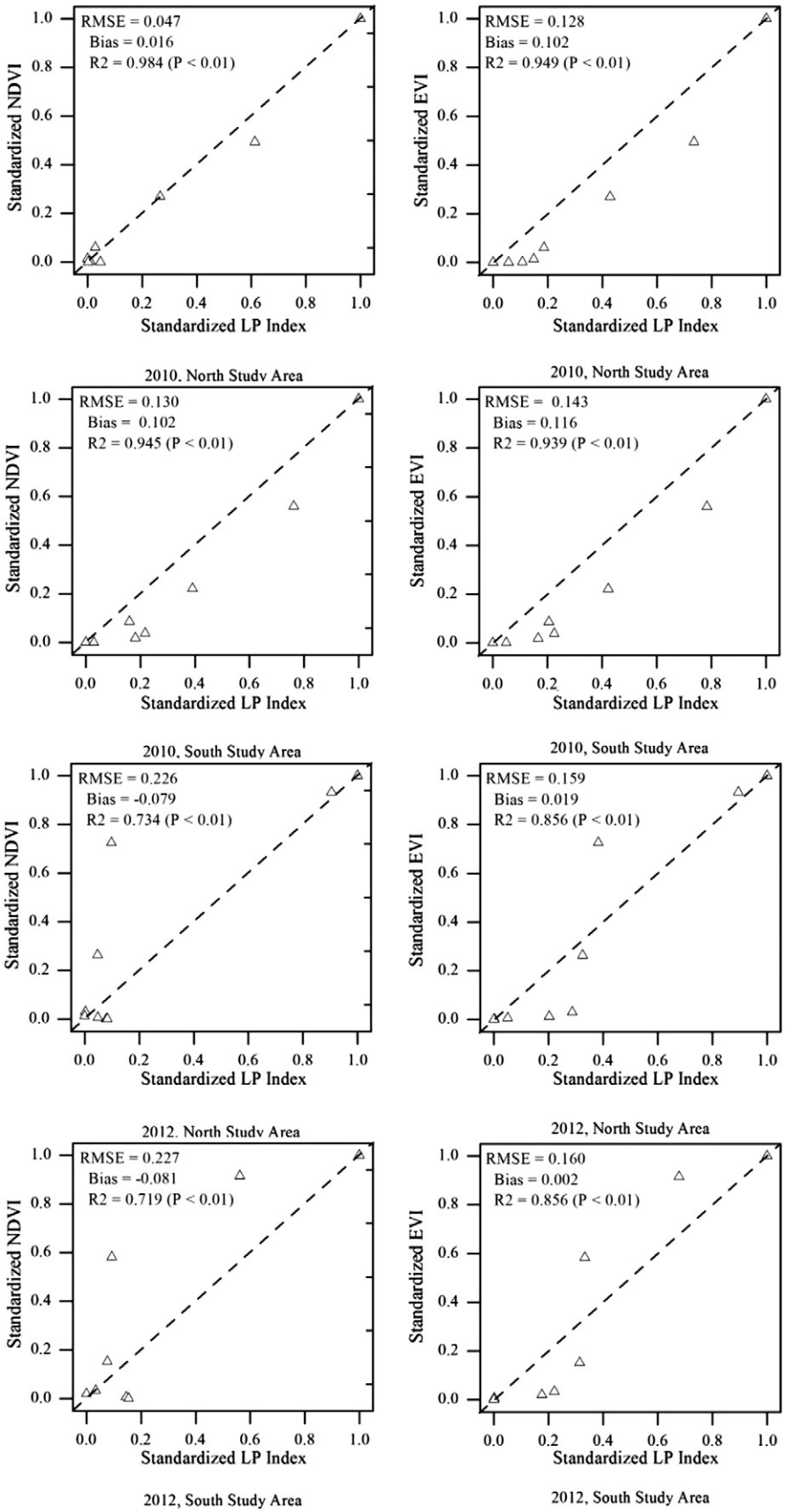

Fig. 4. Comparison of daily VI and landscape phenology (LP) index values for leaf coloration; triangles represent pairs of VI and LP index values; root mean square errors (RMSE), bias, coefficient of determination (R^2), significance level and 1:1 lines are provided. VI values were normalized using the formula: (observation − minimum)/(maximum − minimum). LP index values were normalized using the formula: (observation − minimum)/(maximum − minimum) × (−1) + 1.

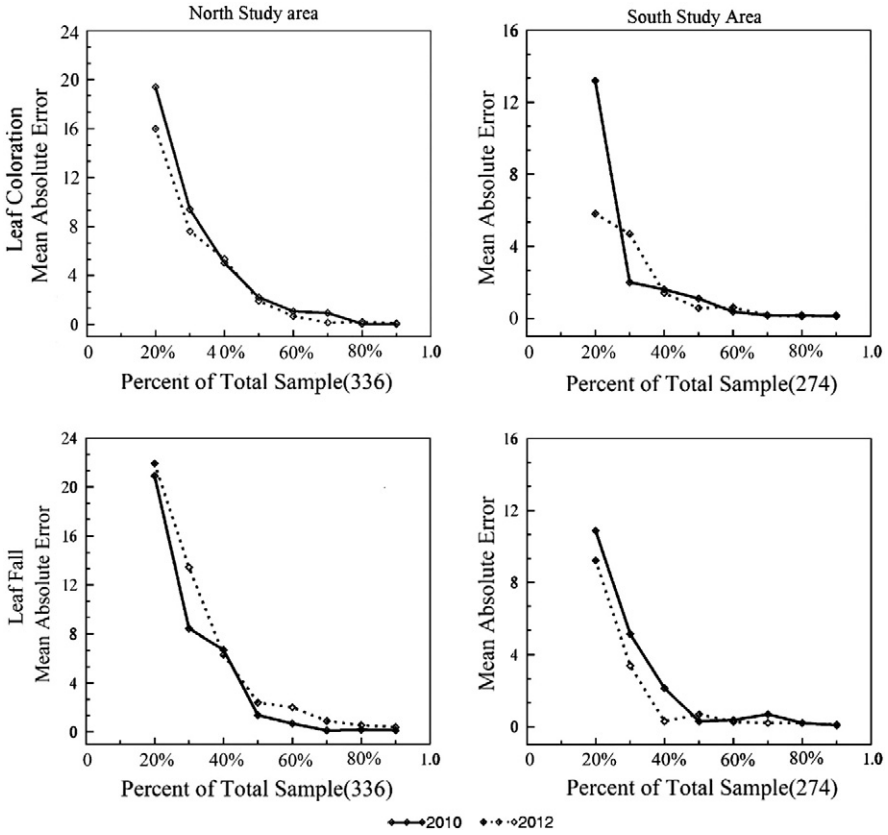

Fig. 5. The sample size effects on LP estimates using 2010 and 2012 leaf coloration and leaf fall time series in the north and south study areas. Each point represents the mean absolute error (MAE) between LP index estimates from a fraction of the total sample (at a given percentage) and the LP index estimates using all available samples (for all days). The value at 10% level was not presented because the MAE was very large.

change is more strongly influenced by leaf coloration than by leaf fall of deciduous trees. Deciduous leaves change color in autumn from green to yellow or red due to chlorophyll degradation and anthocyanin synthesis (Feild, Lee, & Holbrook, 2001; Matile, 2000). Therefore as leaf chlorophyll content declines in autumn, near-infrared reflectance of tree canopies decreases and red reflectance increases, leading to a decline in VI values.

Furthermore, the beginning of LP leaf fall leveling off corresponded to the time when NDVI reached its minimum. This phenomenon is interesting because it may imply that the NDVI minimum reflects landscape-scale full leaf fall in a mixed forest. A slight increase in NDVI following its minimum was observed for most cases, which is probably due to the understory plants with longer growing seasons (Zhu et al., 2012) being exposed as a result of canopies opening up. Meanwhile, EVI declined monotonically into late autumn, with a slightly faster decreasing rate after full leaf fall. This contrast might be due to EVI being more sensitive to forest structure (Pettorelli et al., 2005) and being capable of detecting more reflectance from the understory in addition to canopy trees during the late autumn season. Such hypotheses certainly merit further studies.

Akin to our satellite phenology validation work during the spring season (Liang et al., 2011), it is the first time that the autumn LSP was validated with intensively collected in situ data. The high spatial density and temporal frequency of the ground data allowed for increased landscape representativeness of phenological measurements collected with a traditional observer-based approach. The upscaling technique was necessary for producing a phenological representation at the landscape level as a spatially comparable counterpart of satellite signals. In addition, we used both 16-day standard MODIS VI product and daily MODIS NBAR VI in order to address the temporal resolution limitation noted in earlier work (Liang et al., 2011; Schwartz et al., 2002; Soudani et al., 2008). Although the advantage of using daily data was only partly supported by improved dormancy onset detection in selected cases, the high frequency of both field and satellite data did allow for direct comparison of time series without temporal interpolation, which helped reveal useful details about the relationships of ground phenological processes and vegetation indices, as is the case for spring phenology (Liang et al., 2014).

Overall, we found a clear connection between MODIS-based end of season and ground-based full leaf coloration of deciduous canopies. However, the accuracy of MODIS-based senescence onset (when greenness begins to decline rapidly after the growing season peak) was not evaluated in the current study due to a lack of ground observations during the initial stage of leaf coloration in 2010 and 2012. In a subsequent autumn 2013 field campaign, we started observation a few days earlier (before the onset of leaf yellowing) to facilitate validating senescence onset in future work. Furthermore, MODIS VI data estimated consistently later dormancy onset relative to LP full leaf coloration. This offset may be caused by additional reflectance from freshly fallen leaf litter which delays the VI decline (Nagler, Daughtry, & Goward, 2000; van Leeuwen & Huete, 1996). Such factors may induce a shift of the maximum curvature change point on a logistic curve fitted to VI time series rightward, thus leading to a delayed prediction of dormancy onset date (Hmimina et al., 2013).

Given the spatial and temporal variability of autumn phenology across temperate deciduous broadleaf forests in the eastern United States, similar studies replicated at additional locations are needed for more comprehensive validation of remotely sensed autumn phenology in the future. Our sample size sensitivity analysis suggested that LP estimates from half of the current sample size in our study may still provide comparable accuracy in LP estimates. However, the larger mean absolute error at lower sampling percentage levels may also be contributed by reduced species representativeness. Therefore it is important to consider the species composition of a forest patch when

applying this general guideline to field campaigns in other regions to make sure that all the dominant species in those regions are covered. Our previous work also suggested that at least 20 samples from each species should be included to give a reasonable estimate of population level phenology (Liang et al., 2011). In addition to performing effective high resolution ground observations, alternative measurements such as Landsat data and webcam network records will all be useful to extend the spatial coverage and provide additional perspectives of satellite-based LSP validation. Therefore, an integrated approach combining these different observation means is promising to allow more comprehensive evaluation of LSP over large areas and additional environments.

6. Conclusions

We evaluated the ability of MODIS NDVI and EVI based land surface phenology to track autumn landscape phenology in a temperate mixed forest. In particular, MODIS VI-based dormancy onset was able to estimate LP full leaf coloration with a difference of 0–12 days and a mean absolute error of 5.25 days; and VI time series closely tracked the temporal dynamics of leaf coloration. In addition, minimum NDVI values at later autumn phenological developmental stages closely corresponded with the time of full leaf fall. These findings support the usefulness of MODIS data for monitoring autumn phenology in a mixed forest. The characteristics of autumn phenology are very different than the spring, and it is crucial to understand and more accurately monitor both spring and autumn phenology to constrain changes in the growing season. This study advances our knowledge of autumn phenology as detected by the satellites and on the ground, and validates the utility of coarse resolution land surface phenology during the crucial, but less studied autumn season.

Acknowledgments

We would like to acknowledge Audrey Fusco, Jacquelyn Hurry, and Isaac Park who all contributed to the in situ phenological data collection. We are grateful to the entire staff at the Kemp Natural Resources Station for their support during all of our field campaigns. The authors would also thank the two anonymous reviewers for their helpful comments, and Xiaoyang Zhang for his insight on land surface phenology extraction. This project was supported by the National Science Foundation under grants BCS-0649380, 0937735, and 1157215; and the National Natural Science Foundation of China under grant 41222008.

References

Ahl, D., Gower, S., Burrows, S., Shabanov, N., Myneni, R., & Knyazikhin, Y. (2006). Monitoring spring canopy phenology of a deciduous broadleaf forest using MODIS. *Remote Sensing of Environment*, *104*, 88–95.

Burrows, S., Gower, S., Clayton, M., Mackay, D., Ahl, D., Norman, J.M., et al. (2002). Application of geostatistics to characterize leaf area index (LAI) from flux tower to landscape scales using a cyclic sampling design. *Ecosystems*, *5*, 0667–0679.

Burrows, S., Gower, S., Norman, J., Diak, G., Mackay, D., Ahl, D., et al. (2003). Spatial variability of aboveground net primary production for a forested landscape in northern Wisconsin. *Canadian Journal of Forest Research*, *33*, 2007–2018.

Chen, X.Q., Hu, B., & Yu, R. (2005). Spatial and temporal variation of phenological growing season and climate change impacts in temperate eastern China. *Global Change Biology*, *11*, 1118–1130.

Chen, J., Jonsson, P., Tamura, M., Gu, Z., Matsushita, B., & Eklundh, L. (2004). A simple method for reconstructing a high-quality NDVI time-series data set based on the Savitzky–Golay filter. *Remote Sensing of Environment*, *91*, 332–344.

Clayton, M.K., & Hudelson, B.D. (1995). Confidence intervals for autocorrelations based on cyclic samples. *Journal of the American Statistical Association*, *90*, 753–757.

Cleland, E.E., Chuine, I., Menzel, A., Mooney, H.A., & Schwartz, M.D. (2007). Shifting plant phenology in response to global change. *Trends in Ecology & Evolution*, *22*, 357–365.

Davis, K.J., Bakwin, P.S., Yi, C., Berger, B.W., Zhao, C., Teclaw, R.M., et al. (2003). The annual cycles of CO_2 and H_2O exchange over a northern mixed forest as observed from a very tall tower. *Global Change Biology*, *9*, 1278–1293.

Delbart, N., Kergoat, L., Le Toan, T., Lhermitte, J., & Picard, G. (2005). Determination of phenological dates in boreal regions using normalized difference water index. *Remote Sensing of Environment*, *97*, 26–38.

Denning, A., Nicholls, M., Prihodko, L., Baker, I., Vidale, P.L., Davis, K., et al. (2003). Simulated variations in atmospheric CO_2 over a Wisconsin forest using a coupled ecosystem–atmosphere model. *Global Change Biology*, *9*, 1241–1250.

Desai, A.R., Bolstad, P.V., Cook, B.D., Davis, K.J., & Carey, E.V. (2005). Comparing net ecosystem exchange of carbon dioxide between an old-growth and mature forest in the upper Midwest, USA. *Agricultural and Forest Meteorology*, *128*, 33–55.

Donnelly, A., Salamin, N., & Jones, M.B. (2006). Changes in tree phenology: An indicator of spring warming in Ireland? *Biology and Environment: Proceedings of the Royal Irish Academy*, *106*, 47–55.

Dragoni, D., & Rahman, A.F. (2012). Trends in fall phenology across the deciduous forests of the eastern USA. *Agricultural and Forest Meteorology*, *157*, 96–105.

Dragoni, D., Schmid, H.P., Wayson, C.A., Potter, H., Grimmond, C.S.B., & Randolph, J.C. (2011). Evidence of increased net ecosystem productivity associated with a longer vegetated season in a deciduous forest in south-central Indiana, USA. *Global Change Biology*, *17*, 886–897.

Ewers, B., Mackay, D., Gower, S., Ahl, D., Burrows, S., & Samanta, S. (2002). Tree species effects on stand transpiration in northern Wisconsin. *Water Resources Research*, *38*(8–1), 8–11.

Feild, T.S., Lee, D.W., & Holbrook, N.M. (2001). Why leaves turn red in autumn. The role of anthocyanins in senescing leaves of red-osier dogwood. *Plant Physiology*, *127*, 566–574.

Fisher, J., Mustard, J., & Vadeboncoeur, M. (2006). Green leaf phenology at Landsat resolution: Scaling from the field to the satellite. *Remote Sensing of Environment*, *100*, 265–279.

Ganguly, S., Friedl, M.A., Tan, B., Zhang, X., & Verma, M. (2010). Land surface phenology from MODIS: Characterization of the Collection 5 global land cover dynamics product. *Remote Sensing of Environment*, *114*, 1805–1816.

Hamunyela, E., Verbesselt, J., Roerink, G., & Herold, M. (2013). Trends in spring phenology of western European deciduous forests. *Remote Sensing*, *5*, 6159–6179.

Hmimina, G., Dufrêne, E., Pontailler, J.Y., Delpierre, N., Aubinet, M., Caquet, B., et al. (2013). Evaluation of the potential of MODIS satellite data to predict vegetation phenology in different biomes: An investigation using ground-based NDVI measurements. *Remote Sensing of Environment*, *132*, 145–158.

Holben, B.N. (1986). Characteristics of maximum-value composite images from temporal AVHRR data. *International Journal of Remote Sensing*, *7*, 1417–1434.

Huete, A., Didan, K., Miura, T., Rodriguez, E.P., Gao, X., & Ferreira, L.G. (2002). Overview of the radiometric and biophysical performance of the MODIS vegetation indices. *Remote Sensing of Environment*, *83*, 195–213.

Hufkens, K., Friedl, M., Sonnentag, O., Braswell, B.H., Milliman, T., & Richardson, A.D. (2012). Linking near-surface and satellite remote sensing measurements of deciduous broadleaf forest phenology. *Remote Sensing of Environment*, *117*, 307–321.

Hughes, L. (2000). Biological consequences of global warming: Is the signal already apparent? *Trends in Ecology & Evolution*, *15*, 56–61.

Jeong, S. -J., Ho, C. -H., Gim, H. -J., & Brown, M.E. (2011). Phenology shifts at start vs. end of growing season in temperate vegetation over the Northern Hemisphere for the period 1982–2008. *Global Change Biology*, *17*, 2385–2399.

Jönsson, P., & Eklundh, L. (2002). Seasonality extraction by function fitting to time-series of satellite sensor data. *IEEE Transactions on Geoscience and Remote Sensing*, *40*, 1824–1832.

Julien, Y., & Sobrino, J. (2009). Global land surface phenology trends from GIMMS database. *International Journal of Remote Sensing*, *30*, 3495–3513.

Kaduk, J.D., & Heimann, M. (1996). A prognostic phenology scheme for global terrestrial carbon cycle models. *Climate Research*, *6*, 1–19.

Kang, S., Running, S., Lim, J., Zhao, M., Park, C., & Loehman, R. (2003). A regional phenology model for detecting onset of greenness in temperate mixed forests, Korea: An application of MODIS leaf area index. *Remote Sensing of Environment*, *86*, 232–242.

Kovalskyy, V., Roy, D.P., Zhang, X.Y., & Ju, J. (2012). The suitability of multi-temporal web-enabled Landsat data NDVI for phenological monitoring—A comparison with flux tower and MODIS NDVI. *Remote Sensing Letters*, *3*, 325–334.

Liang, L., & Schwartz, M.D. (2009). Landscape phenology: An integrative approach to seasonal vegetation dynamics. *Landscape Ecology*, *24*, 465–472.

Liang, L., Schwartz, M.D., & Fei, S.L. (2011). Validating satellite phenology through intensive ground observation and landscape scaling in a mixed seasonal forest. *Remote Sensing of Environment*, *115*, 143–157.

Liang, L., Schwartz, M.D., Wang, Z., Gao, F., Schaaf, C., Tan, B., et al. (2014). A cross-comparison of spatiotemporally enhanced springtime phenological measurements from satellites and ground in a northern U.S. mixed forest. *IEEE Transactions on Geoscience and Remote Sensing*, *52*, 7513–7752.

Liu, L., Liu, L., Liang, L., Donnelly, A., Park, I., & Schwartz, M. D. (2014). Effects of elevation on spring phenological sensitivity to temperature in Tibetan Plateau grasslands. *Chinese Science Bulletin*, *59*, 4856–4863.

Matile, P. (2000). Biochemistry of Indian summer: Physiology of autumnal leaf coloration. *Experimental Gerontology*, *35*, 145–158.

Meier, U. (2001). *Growth stages of mono- and dicotyledonous plants*. BBCH monograph. Berlin: German federal biological research centre for agriculture and forestry.

Melaas, E.K., Friedl, M.A., & Zhu, Z. (2013). Detecting interannual variation in deciduous broadleaf forest phenology using Landsat TM/ETM+ data. *Remote Sensing of Environment*, *132*, 176–185.

Menzel, A. (2000). Trends in phenological phases in Europe between 1951 and 1996. *International Journal of Biometeorology*, *44*, 76–81.

Morisette, J., Privette, J.L., & Justice, C.O. (2002). A framework for the validation of MODIS Land products. *Remote Sensing of Environment*, *83*, 77–96.

Moulin, S., Kergoat, L., Viovy, N., & Dedieu, G. (1997). Global-scale assessment of vegetation phenology using NOAA/AVHRR satellite measurements. *Journal of Climate*, *10*, 1154–1170.

Myneni, R., Keeling, C., Tucker, C., Asrar, G., & Nemani, R. (1997). Increased plant growth in the northern high latitudes from 1981 to 1991. *Nature*, *386*, 698–702.
Nagler, P.L., Daughtry, C.S.T., & Goward, S.N. (2000). Plant litter and soil reflectance. *Remote Sensing of Environment*, *71*, 207–215.
Peñuelas, J., Filella, I., & Comas, P. (2002). Changed plant and animal life cycles from 1952 to 2000 in the Mediterranean region. *Global Change Biology*, *8*, 531–544.
Pettorelli, N., Vik, J.O., Mysterud, A., Gaillard, J. -M., Tucker, C.J., & Stenseth, N.C. (2005). Using the satellite-derived NDVI to assess ecological responses to environmental change. *Trends in Ecology & Evolution*, *20*, 503–510.
Piao, S., Friedlingstein, P., Ciais, P., Viovy, N., & Demarty, J. (2007). Growing season extension and its impact on terrestrial carbon cycle in the Northern Hemisphere over the past 2 decades. *Global Biogeochemical Cycles*, *21*, GB3018.
Richardson, A. D., Andy Black, T., Ciais, P., Delbart, N., Friedl, M., Gobron, N., et al. (2010). Influence of spring and autumn phenological transitions on forest ecosystem productivity. *Philosophical Transactions of the Royal Society, B: Biological Sciences*, *365*, 3227–3246.
Richardson, A.D., Bailey, A.S., Denny, E.G., Martin, C.W., & O'Keefe, J. (2006). Phenology of a northern hardwood forest canopy. *Global Change Biology*, *12*, 1174–1188.
Richardson, A. D., Friedl, M., Frolking, S., Pless, R., & Collaborators, P. (2011). PhenoCam: A continental-scale observatory for monitoring the phenology of terrestrial vegetation. *AGU fall, meeting abstracts* (B11D-0517).
Schaaf, C., Gao, F., Strahler, A.H., Lucht, W., Li, X., Tsang, T., et al. (2002). First operational BRDF, albedo nadir reflectance products from MODIS. *Remote Sensing of Environment*, *83*, 135–148.
Schaaf, C., Liu, J., Gao, F., & Strahler, A.H. (2011). Aqua and Terra MODIS albedo and reflectance anisotropy products. *Land Remote Sensing and Global Environmental Change*, *11*, 549–561.
Schwartz, M.D. (1997). Spring index models: An approach to connecting satellite and surface phenology. *Phenology in Seasonal Climates I*, 23–38.
Schwartz, M.D. (1999). Advancing to full bloom: Planning phenological research for the 21st century. *International Journal of Biometeorology*, *42*, 113–118.
Schwartz, M. D., & Reed, B. C. (1999). Surface phenology and satellite sensor-derived onset of greenness: An initial comparison. *International Journal of Remote Sensing*, *20*, 3451–3457.
Schwartz, M.D., Hanes, J.M., & Liang, L. (2013). Comparing carbon flux and high-resolution spring phenological measurements in a northern mixed forest. *Agricultural and Forest Meteorology*, *169*, 136–147.
Schwartz, M. D., Reed, B., & White, M. (2002). Assessing satellite-derived start-of-season measures in the conterminous USA. *International Journal of Climatology*, *22*, 1793–1805.
Shuai, Y., Schaaf, C., Zhang, X., Strahler, A., Roy, D., Morisette, J., et al. (2013). Daily MODIS 500 m reflectance anisotropy direct broadcast DB products for monitoring vegetation phenology dynamics. *International Journal of Remote Sensing*, *34*, 5997–6016.
Sonnentag, O., Hufkens, K., Teshera-Sterne, C., Young, A.M., Friedl, M., Braswell, B.H., et al. (2012). Digital repeat photography for phenological research in forest ecosystems. *Agricultural and Forest Meteorology*, *152*, 159–177.
Soudani, K., Hmimina, G., Delpierre, N., Pontailler, J.Y., Aubinet, M., Bonal, D., et al. (2012). Ground-based network of NDVI measurements for tracking temporal dynamics of canopy structure and vegetation phenology in different biomes. *Remote Sensing of Environment*, *123*, 234–245.
Soudani, K., le Maire, G., Dufrêne, E., François, C., Delpierre, N., Ulrich, E., et al. (2008). Evaluation of the onset of green-up in temperate deciduous broadleaf forests derived from Moderate Resolution Imaging Spectroradiometer (MODIS) data. *Remote Sensing of Environment*, *112*, 2643–2655.
Taylor, G., Tallis, M.J., Giardina, C.P., Percy, K.E., Miglietta, F., Gupta, P.S., et al. (2008). Future atmospheric CO_2 leads to delayed autumnal senescence. *Global Change Biology*, *14*, 264–275.
van Leeuwen, W.J.D., & Huete, A.R. (1996). Effects of standing litter on the biophysical interpretation of plant canopies with spectral indices. *Remote Sensing of Environment*, *55*, 123–138.
Viovy, N., Arino, O., & Belward, A. (1992). The Best Index Slope Extraction (BISE): A method for reducing noise in NDVI time-series. *International Journal of Remote Sensing*, *13*, 1585–1590.
Wang, Z., Schaaf, C., Chopping, M.J., Strahler, A.H., Wang, J., Román, M.O., et al. (2012). Evaluation of Moderate-Resolution Imaging Spectroradiometer (MODIS) snow albedo product (MCD43A) over tundra. *Remote Sensing of Environment*, *117*, 264–280.
Wang, Z., Schaaf, C., Strahler, A.H., Chopping, M.J., Román, M.O., Shuai, Y., et al. (2014). Evaluation of MODIS albedo product (MCD43A) over grassland, agriculture and forest surface types during dormant and snow-covered periods. *Remote Sensing of Environment*, *140*, 60–77.
White, M., de Beurs, K., Didan, K., Inouye, D., Richardson, A., Jensen, O., et al. (2009). Intercomparison, interpretation, and assessment of spring phenology in North America estimated from remote sensing for 1982–2006. *Global Change Biology*, *15*, 2335–2359.
White, K., Pontius, J., & Schaberg, P. (2014). Remote sensing of spring phenology in northeastern forests: A comparison of methods, field metrics and sources of uncertainty. *Remote Sensing of Environment*, *148*, 97–107.
White, M., Thornton, P.E., & Running, S.W. (1997). A continental phenology model for monitoring vegetation responses to interannual climatic variability. *Global Biogeochemical Cycles*, *11*, 217–234.
Wolfe, R.E., Roy, D.P., & Vermote, E. (1998). MODIS Land data storage, gridding, and compositing methodology: Level 2 grid. *IEEE Transactions on Geoscience and Remote Sensing*, *36*, 1324–1338.
Wu, C., Chen, J.M., Black, T.A., Price, D.T., Kurz, W.A., Desai, A.R., et al. (2013). Interannual variability of net ecosystem productivity in forests is explained by carbon flux phenology in autumn. *Global Ecology and Biogeography*, *22*, 994–1006.
Wu, C., Gough, C.M., Chen, J.M., & Gonsamo, A. (2013). Evidence of autumn phenology control on annual net ecosystem productivity in two temperate deciduous forests. *Ecological Engineering*, *60*, 88–95.
Wu, C., Niu, Z., & Gao, S. (2010). Gross primary production estimation from MODIS data with vegetation index and photosynthetically active radiation in maize. *Journal of Geophysical Research*, *115*, D12127.
Zhang, X. (2001). Global vegetation phenology from AVHRR and MODIS data. *IEEE International Geoscience and Remote Sensing Symposium*, *5*, 2262–2264.
Zhang, X., Friedl, M., & Schaaf, C. (2006). Global vegetation phenology from moderate resolution imaging spectroradiometer (MODIS): Evaluation of global patterns and comparison with in situ measurements. *Journal of Geophysical Research*, *111*, G04017.
Zhang, X., Friedl, M., Schaaf, C., Strahler, A., Hodges, J., Gao, F., et al. (2003). Monitoring vegetation phenology using MODIS. *Remote Sensing of Environment*, *84*, 471–475.
Zhang, X., & Goldberg, M.D. (2011). Monitoring fall foliage coloration dynamics using time-series satellite data. *Remote Sensing of Environment*, *115*, 382–391.
Zhang, X., Tan, B., & Yu, Y. (2014). Interannual variations and trends in global land surface phenology derived from enhanced vegetation index during 1982–2010. *International Journal of Biometeorology*, *58*, 547–564.
Zhu, W.Q., Tian, H.Q., Xu, X.F., Pan, Y., Chen, G., & Lin, W. (2012). Extension of the growing season due to delayed autumn over mid and high latitudes in North America during 1982–2006. *Global Ecology and Biogeography*, *21*, 260–271.